



## Platelet lysate coating on scaffolds directly and indirectly enhances cell migration, improving bone and blood vessel formation



Julie Leotot<sup>a,b</sup>, Laura Coquelin<sup>a,b</sup>, Gwellaouen Bodivit<sup>a,b</sup>, Philippe Bierling<sup>a,b</sup>, Philippe Hernigou<sup>a,c</sup>, Helene Rouard<sup>a,b,d</sup>, Nathalie Chevallier<sup>a,b,\*</sup>

<sup>a</sup> Université Paris-Est, Faculté de Médecine, Laboratoire de "Bioingénierie Cellulaire, Tissulaire et Sanguine", EA3952 Créteil, France

<sup>b</sup> Etablissement Français du Sang d'Ile-de-France, Unité d'Ingénierie et de Thérapie Cellulaire, Créteil, France

<sup>c</sup> Service de Chirurgie Orthopédique et Traumatologique, AP-HP Hôpital Henri-Mondor, Créteil, France

<sup>d</sup> AP-HP Hôpital Henri-Mondor – A, Chenevier, Service Hospitalier, Créteil, France

### ARTICLE INFO

#### Article history:

Received 9 October 2012

Received in revised form 28 December 2012

Accepted 1 February 2013

Available online 9 February 2013

#### Keywords:

Bone tissue engineering

Chemotaxis

Hydroxyapatite coating

Platelet lysate

Mesenchymal stromal cell

### ABSTRACT

Suitable colonization and vascularization of tissue-engineered constructs after transplantation represent critical steps for the success of bone repair. Human platelet lysate (hPL) is composed of numerous growth factors known for their proliferative, differentiative and chemo-attractant effects on various cells involved in wound healing and bone growth. The aim of this study was to determine whether the delivery of human mesenchymal stromal cells (hMSC) seeded on hPL-coated hydroxyapatite/ $\beta$ -tricalcium phosphate (HA/ $\beta$ -TCP) scaffolds could enhance vascularization and bone formation, as well as to investigate the mechanisms by which hMSC participate in tissue regeneration. Our study demonstrates that hPL can be coated on HA/ $\beta$ -TCP scaffolds, which play direct and indirect effects on implanted and/or resident stem cells. Effectively, we show that hPL coating directly increases chemo-attraction to and adhesion of hMSC and endothelial cells on the scaffold. Moreover, we show that hPL coating induces hMSC to produce and secrete pro-angiogenic proteins (placental growth factor and vascular endothelial growth factor) which allow the proliferation and specific chemo-attraction of endothelial cells in vitro, thus improving in vivo neovascularization and new bone formation. This study highlights the potential of functionalizing biomaterials with hPL and shows that this growth factor combination can have synergistic effects leading to enhanced bone and blood vessel formation.

© 2013 Acta Materialia Inc. Published by Elsevier Ltd. All rights reserved.

### 1. Introduction

Large bone defect repair following trauma, pathology or tumor resection presents significant clinical challenges for reconstructive and orthopaedic surgery [1–3]. One common surgical procedure is autologous bone grafting. However, this procedure is associated with potential complications, including chronic pain and risk of infection, as well as being limited by the amount of available bone. This has led to a search for alternative methods using bone substitutes.

Bone tissue engineering using osteoprogenitor cells such as human mesenchymal stromal cells (hMSC) combined with a three-dimensional (3-D) scaffold represents a promising therapeutic approach and provides an alternative to autologous bone grafting for the treatment of bone defects. Several scaffolds are currently available, of either natural or synthetic origin. The combination

of these biomaterials with hMSC has been shown to be efficient in the repair of large bone defects in several experimental animal models [4–6].

Nevertheless, bone regeneration is a complex and coordinated physiological process involving a number of molecular, cellular, biochemical and mechanical mechanisms [7–9]. Angiogenesis and osteogenesis are closely related, since the development of a functional microvascular network is an essential prerequisite for successful bone formation [10–13]. A lack of blood vessels in grafted sites is a major issue affecting cell survival and proliferation failure [14]. Indeed, the formation of new vessels is required not only for oxygen, nutrient and soluble factor supply, but also to provide a communicative network between the implant and neighbouring tissues. This vascularization allows scaffold integration with the surrounding host tissues and mobilization of resident cells.

A variety of molecules involved in neo-angiogenesis and osteogenesis have been used to functionalize scaffolds, such as fibroblast growth factor (FGF), insulin-like growth factor (IGF)-1, transforming growth factor (TGF)- $\beta$ 1, vascular endothelial growth factor

\* Corresponding author at: Etablissement Français du Sang d'Ile-de-France, Unité d'Ingénierie et de Thérapie Cellulaire, Créteil, France. Tel.: +33 1 56 72 21 20; fax: +33 1 56 72 21 23.

E-mail address: [nathalie.chevallier@efs.sante.fr](mailto:nathalie.chevallier@efs.sante.fr) (N. Chevallier).

(VEGF) and bone morphogenic proteins (BMPs) [15–19]. These findings demonstrate that a combination of factors further increases bone regeneration compared with single factor stimulation [16,17]. However, a universally applicable combination of growth factors has yet to be established for bone cell therapy.

Platelets contain many growth factors, including platelet-derived growth factor (PDGF), FGF, IGF, platelet-derived angiogenesis factor (PDAF), TGF- $\beta$ , platelet factor 4 (PF-4), platelet-derived epidermal growth factor (PDEGF) and VEGF [20,21]. These growth factors are known for their growth, differentiative and chemo-attractant effects on various cells, like hMSC and endothelial progenitor cells (EPC) [22,23]. Taking into consideration that tissue regeneration involves complex cellular interactions regulated by multiple signals, a combination of a number of these factors could have additive or even synergistic effects leading to enhanced bone and blood vessel formation.

Platelets have been used in therapeutic applications in maxillo-facial, oral, plastic and orthopaedic surgery. Their application is in the form of either: (i) platelet-rich plasma (PRP), obtained by concentrating platelets by gradient density centrifugation; (ii) platelet gel (PLG), obtained by treatment of PRP with thrombin, a process known to release bioactive molecules; (iii) releasates prepared from PRP, also called platelet lysate (PL). In combination with autologous bone grafts PRP and PLG have been shown to accelerate bone formation and bone density [24–31], in addition to enhancing revascularization when combined with bone marrow stromal cells [32]. These promising case reports demonstrate the usefulness of platelets for a wide range of clinical applications to improve healing after surgical procedures. In addition, PL obtained by freezing platelets has been demonstrated to deliver more growth factors compared with PRP after aggregation [33]. Recently human PL (hPL) has been suggested as a culture supplement for the expansion and clinical grade production of hMSC [22,33–35] and EPC [36]. Furthermore, we have previously shown that hPL medium can prime hMSC differentiation towards the osteoblastic lineage, which enhances *in vivo* bone regeneration [22]. A recent study has reported that MSC and PL in a fibrin or collagen scaffold can promote new bone formation around an uncemented hip prosthesis [37]. However, these scaffolds are unsuitable for filling large bone defects. To our knowledge no study has investigated the feasibility of coating a bone graft substitute with hPL use in the treatment of large bone defects. Moreover, the mechanisms by which hMSC seeded on hPL-coated hydroxyapatite/ $\beta$ -tricalcium phosphate (HA/ $\beta$ -TCP) scaffolds induce tissue repair have never been addressed.

The aim of this study was to determine whether the functionalization of HA/ $\beta$ -TCP scaffolds with hPL, before seeding them with hMSC, could enhance vascularization and bone formation, as well as to investigate the mechanisms by which hMSC participate in tissue regeneration. For this study hMSC were cultured in the absence of osteogenic agents in standard growth medium complemented with foetal bovine serum (FBS) to exclusively evaluate the impact of the hPL coating. The effect of hPL-coated HA/ $\beta$ -TCP scaffolds on chemo-attraction, adhesion, morphology, distribution, gene expression and protein secretion of hMSC was first evaluated *in vitro*. Then the effects on neovascularization and new bone formation *in vivo* in a mouse model were studied.

## 2. Materials and methods

### 2.1. Mesenchymal stromal cell cultures

hMSC were isolated from bone marrow (3–5 ml) collected from the iliac crest of patients undergoing standard bone marrow transplantation procedures (AP-HP Hôpital Henri Mondor, Créteil, France), after having received their informed consent. Bone

marrow aspirates from three healthy donors (15–26 years old) were used. Nucleated cells from fresh bone marrow were seeded at  $2 \times 10^5$  cells  $\text{cm}^{-2}$  in 225  $\text{cm}^2$  flasks. hMSC were expanded in  $\alpha$ -modified Eagle's medium ( $\alpha$ MEM) (PAA, Les Mureaux, France) supplemented with 10% FBS (StemCell Technologies, Grenoble, France) and 0.5% ciprofloxacin (Bayer Pharma, Puteaux, France). The cultures were maintained in a humidified atmosphere with 5%  $\text{CO}_2$  at 37 °C and the culture medium was changed twice a week. Upon reaching 80% confluence adherent cells were detached using  $1 \times$  trypsin/EDTA (PAA, Les Mureaux, France) and replated at a density of  $10^3$  cells  $\text{cm}^{-2}$  (passage 1). Cell samples were used to confirm the hMSC characteristics as previously described [22]. Briefly, all the hMSC used in this study were positive for CD90 (clone 5E10), CD105 (clone 266), CD73 (clone AD2) (all from Becton Dickinson and Co., Franklin Lakes, NJ) and negative for CD34 (clone AC136, Miltenyi Biotec, Bergsch Gladbach, Germany) and CD45 (clone 2D1, Becton Dickinson), and were able to differentiate along the osteogenic, chondrogenic and adipogenic lineages (data not shown).

### 2.2. Endothelial cell cultures

Human umbilical vein endothelial cells (hUVEC), provided by the team of Dr Llorens-Cortes of the Collège de France (Paris, France), were cultured in Endothelial Cell Growth Medium 2 (PromoCell, Heidelberg, Germany).

Human bone marrow endothelial cells [38], provided by the laboratory of Dr Li of the Université Paris 6 (Paris, France), were cultured in  $\alpha$ MEM with 10% FBS.

Endothelial cell cultures were maintained in a humidified atmosphere with 5%  $\text{CO}_2$  at 37 °C and the culture medium was changed twice a week.

### 2.3. Platelet lysate preparation

hPL was obtained from platelet apheresis collections performed at the Etablissement Français du Sang (Rungis, France). All apheresis products were biologically qualified in accordance with French legislation. The platelet count in each product was measured automatically with an ABXpenta 60C<sup>+</sup> (Horiba ABX, Montpellier, France). A minimum of four different batches were mixed to adjust the concentration to  $10^9$  platelets  $\text{ml}^{-1}$ , frozen at –80 °C and subsequently used to obtain hPL containing platelet-released growth factors. Remaining platelet bodies were eliminated by centrifugation at 1400g.

### 2.4. Biomaterial coating and cell seeding

The HA (65%)/ $\beta$ -TCP (35%) scaffolds, provided by Ceraver (Roissy, France), had an average porosity of  $65 \pm 5\%$  ( $60 \pm 5\%$  macroporosity and  $40 \pm 5\%$  microporosity) and a specific surface area of  $0.8 \text{ m}^2 \text{ g}^{-1}$ . The granules had a diameter of 2–3 mm and weighed  $8.0 \pm 1 \text{ mg}$ . These scaffolds were coated by immersion in hPL (hPL-coated) or left uncoated by immersion in  $\alpha$ MEM (control group) in untreated 96-well culture plates at 37 °C overnight. After rinsing in  $1 \times$  HBSS (PAA) they were loaded with  $3 \times 10^5$  hMSC or endothelial cells for 3 h. These seeded constructs were then directly placed into untreated 24-well culture plates and cultured in  $\alpha$ MEM with 10% FBS at 37 °C for 7 days. Cell-free scaffolds were incubated under similar conditions and served as controls.

### 2.5. Evaluation of cell number by DNA quantification

Cell seeding efficiency was determined using an indirect method. After 3 h contact with  $3 \times 10^5$  hMSC or endothelial cells the scaffold was removed and cells that were not adherent on the bone

**Table 1**

Primers used for RT-qPCR of human and mouse genes.

A. References of primers used for RT-qPCR of human genes (TaqMan <sup>®</sup> , Applied Biosystems):	
glyceraldehyde 3-phosphate dehydrogenase (GAPDH)	Hs99999905-m1
osteocalcin (OC)	Hs00960942-m1
osteopontin (OP)	Hs00609452-g1
bone sialoprotein 2 (IBSP)	Hs00173720-m1
bone morphogenetic protein 2 (BMP2)	Hs00154192-m1
vascular endothelial growth factor A (VEGF-A)	Hs00900054-m1
B. Sequences of primers used for RT-qPCR of mouse genes (SYBR <sup>®</sup> Green, Applied Biosystems):	
glyceraldehyde 3-phosphate dehydrogenase (GAPDH)	F 5'-aacttggcattgtggaagg-3' R 5'-ggatgcaggatgatgttct-3'
platelet endothelial cell adhesion molecule 1 (PECAM1)	F 5'-agagacggtcttctcgcagt-3' R 5'-tactggccttcagagcatt-3'

substitute were quantified by determining the DNA content using a Quant-it Picogreen<sup>®</sup> kit (Invitrogen Life Technologies, Villebon sur Yvette, France). Next the number of cells adherent on the bone substitute was deduced by subtraction from the initially seeded cell number. Briefly, remaining cells at the bottom of the wells were lysed in Tris-EDTA (TE) + 0.1% Triton X-100 and digested with 0.2 mg ml<sup>-1</sup> proteinase K solution (Invitrogen) for 12 h at 52 °C. Then the suspension was subjected to a succession of three heat shocks, followed by sonication of the lysates for 10 min. At the same time a standard cell range from 0 to 3 × 10<sup>5</sup> cells was prepared. DNA samples were labelled with Picogreen<sup>®</sup> solution, which only binds double-stranded DNA. After 10 min incubation in the dark the fluorescence was read at 520 nm using a Victor X3 spectrophotometer (PerkinElmer, Courtaboeuf, France). The standard curve was then used to quantify the cells.

## 2.6. Scanning electron microscopy (SEM)

For SEM the specimens were fixed by immersion in 2.5% glutaraldehyde buffer at 4 °C overnight. Scaffolds were then dehydrated in increasing concentrations of ethanol (70–100%), with dehydration being completed using hexamethyldisilazane treatment (Sigma Aldrich, Saint Quentin Fallavier, France). Finally, the samples were air dried, sputtered with a nano-gold film and imaged with a JSM-6301F scanning electron microscope (JEOL, Croissy-sur-Seine, France) at the Laboratoire Interuniversitaire des Systèmes Atmosphériques, Université Paris-Est (Créteil, France).

## 2.7. Cell migration assay

Cell migration was assessed by Boyden chamber assay, using a 6.5 mm Transwell<sup>®</sup> with 0.8 µm pore polycarbonate membrane insert (Corning Life Sciences, Amsterdam, The Netherlands). The inserts were pre-coated with 0.1% gelatin and the cells were serum deprived, washed 2 times in HBSS then placed in αMEM with 0.25% human albumin (Octapharma, Boulogne-Billancourt, France) overnight. Trypsinized cells were resuspended and seeded in the upper chamber (5 × 10<sup>4</sup> hUVEC per insert or 2 × 10<sup>5</sup> hMSC per insert). HA/β-TCP scaffolds, hPL-coated or uncoated, or conditioned medium was placed in the lower chamber. Each chamber was incubated at 37 °C (6 h for hUVEC and 12 h for hMSC). The number of cells crossing the membrane was determined by metabolic activity assay (see below) and staining with 4',6'-diamidino-2-phenylindole (DAPI) (Sigma Aldrich). Cells that both migrated through the membrane and adhered to the scaffold were identified by immunohistochemical staining using human β2-microglobulin (see below).

## 2.8. Metabolic activity assay

Metabolic activity was quantified using alamarBlue<sup>®</sup> reagent (Invitrogen), as described by the manufacturer. Briefly, cells were

exposed to alamarBlue<sup>®</sup> over a period of 3 h and the fluorescence read at 590 nm with a Victor X3 spectrophotometer.

## 2.9. Quantitative real time reverse transcription polymerase chain reaction (RT-qPCR)

Total mRNA was isolated using an RNeasy mini kit (Qiagen, Courtaboeuf, France) or the TRIzol<sup>®</sup> reagent method (Invitrogen) as described by the manufacturers. DNase-treated RNA was reverse transcribed with SuperScript<sup>®</sup> III reverse transcriptase (Invitrogen), the cDNA obtained was amplified using TaqMan<sup>®</sup> or SYBR<sup>®</sup>Green chemistry (Applied Biosystems Life Technologies, Courtaboeuf, France), and monitored with a 7500HT Fast Real-Time PCR System (Applied Biosystems). Primers used for RT-qPCR are listed in Table 1. Amounts of the cDNA of interest were normalized to that of glyceraldehyde 3-phosphate dehydrogenase (GAPDH) ( $\Delta C_t = C_t \text{ gene of interest} - C_t \text{ GAPDH}$ ). Results are reported as relative gene expression ( $2^{-\Delta C_t}$ ).

## 2.10. Multiple protein assay

The composition of hPL was determined using simultaneous quantitative determination of multiple human protein biomarkers, performed by bead-based multiplex analysis (Table 2). A Human Angiogenesis MultiAnalyte Profiling Base Kit A (R&D Systems, Lille, France) and Human Bone Panel 1B Kit (Millipore, Molsheim, France) were used for this assay, as described by the respective manufacturers. This technology was also used to determine the amounts of proteins secreted by hMSC in conditioned medium harvested 7 days after colonization of HA/β-TCP scaffolds. Cell-free scaffolds, hPL-coated or uncoated, were used to deduce the background. Analysis of samples was carried out using a Bio-Plex<sup>™</sup> 200 system (Bio-Rad Laboratories, Hercules, CA) in the immunomonitoring platform of the Institut Mondor de Recherche Biomédicale (Créteil, France).

## 2.11. Animal model and implantation procedures

All animal procedures were approved by the local ethics committee (approval no. 94-612) and conducted in accordance with the European Guidelines for Animal Care (Directive 2010/63/EU). Six SCID mice (males, 7 weeks old) purchased from Charles River Laboratories (Chatillon, France) were used in this experiment. The mice were anaesthetized with isofluran and six subcutaneous dorsal pockets (0.5 cm incisions) were prepared in each one. One hPL-coated or uncoated HA/β-TCP scaffold, containing or not containing hMSC, was implanted in each pocket and the skin closed with 5-0 sutures (Ethicon, San Lorenzo, PR). After either 2 or 7 weeks the animals were killed with an overdose of pentobarbital. The samples were excised and immediately placed in RNA lysis buffer (2 weeks) or 70% ethanol (7 weeks).

**Table 2**  
Analytes for bead-based multiplex analyses.

Human Angiogenesis Base Kit A (R&D Systems)	
ANG	Angiogenin
ANGPT-1	Angiopoietin-1
Endostatin	Endostatin
aFGF	Acid fibroblast growth factor
bFGF	Basic fibroblast growth factor
PIGF	Placental growth factor
PDGF-AA	Platelet-derived growth factor AA
PDGF-BB	Platelet-derived growth factor BB
THBS-2	Thrombospondin 2
VEGF	Vascular endothelial growth factor
VEGF-D	Vascular endothelial growth factor D
Human Bone Panel 1B Kit (Millipore)	
IL-1β	interleukin 1 beta
IL-6	interleukin 6
OPG	osteoprotegerin
OC	osteocalcin
OP	osteopontin
LPTN	leptin
PTH	parathyroid hormone
TNF-α	tumor necrosis factor alpha
ACTH	adrenocorticotrophic hormone
ADPN	adiponectin
INS	insulin

### 2.12. Histological and immunohistochemical assessment

Histological analysis of *in vivo* new bone formation was performed after sample decalcification. 3 μm thick paraffin-embedded cross-sections were then treated with Masson's Trichrome stain.

Immunohistochemical analysis of cell adhesion was performed 24 h after cell seeding and paraffin embedding. To detect hMSC sections were treated with haematoxylin nuclear stain (Sigma Aldrich). Immunohistochemical analysis of chemotaxis was performed after hMSC migration through the membrane. To detect the presence of hMSC on HA/β-TCP scaffolds specimens were treated with rabbit polyclonal anti-human β2-microglobulin followed by biotinylated goat anti-rabbit IgG antibodies (Abcam, Paris, France). Immunostaining was amplified using a peroxidase-conjugated streptavidin complex and peroxidase was detected using DAB substrate (Abcam).

Images were visualized by standard light microscopy and captured using a UC30 digital color camera and CellSens Entry software (Olympus, Rungis, France).

### 2.13. Statistical analysis

All *in vitro* experiments were performed with hMSC derived from bone marrow of three different donors, but only one donor for the *in vivo* study ( $n = 8$  scaffolds per condition). For DNA quantification  $n = 6$  scaffolds per condition, while for quantitative PCR, protein assay and cell migration  $n = 2$  scaffolds per condition was used. Analyses were performed in duplicate for each sample. Comparisons between the two experimental conditions (hPL-coated and uncoated) were performed using the unpaired non-parametric Mann–Whitney *U*-test using GraphPad Prism5 software. A *p* value  $\leq 0.05$  was considered to be statistically significant.

## 3. Results

### 3.1. Determination of hPL protein content

Determination of hPL protein content using bead-based multiplex analyses (Table 2 and Fig. 1) revealed the presence of pro-angiogenic proteins such as PDGF-AA ( $19,596 \pm 10,858$  pg ml<sup>-1</sup>), PDGF-BB ( $22,329 \pm 124$  pg ml<sup>-1</sup>), angiopoietin-1 ( $119,666 \pm 6,049$  pg ml<sup>-1</sup>), angiogenin ( $2,739 \pm 79$  pg ml<sup>-1</sup>) and VEGF-D ( $3,706 \pm 201$  pg ml<sup>-1</sup>). Other pro-angiogenic proteins were detected but in small amounts, such as aFGF, bFGF and VEGF ( $172 \pm 23$ ,  $356 \pm 20$  and  $140 \pm 8$  pg ml<sup>-1</sup>, respectively). Some anti-angiogenic proteins were also present, such as thrombospondin 2 (THBS-2) ( $11,625 \pm 923$  pg ml<sup>-1</sup>) and endostatin ( $25,862 \pm 1,003$  pg ml<sup>-1</sup>). Moreover, this analysis highlighted the presence of proteins which play a role in bone metabolism, such as osteocalcin (OC) ( $3,916 \pm 1,277$  pg ml<sup>-1</sup>), osteopontin (OP) ( $6,963 \pm 448$  pg ml<sup>-1</sup>), and (ADPN) (out of range). Some of them were barely detectable, for example (OPG), (INS) and (LPTN) ( $227 \pm 37$ ,  $147 \pm 6$  and  $500 \pm 7$  pg ml<sup>-1</sup>, respectively). Other proteins were measured in trace amounts. This analysis did not reveal the expression of proteins involved in inflammation. All these data confirm that hPL contains numerous growth factors implicated in angiogenesis and bone remodelling that may play an important role in bone tissue repair.

### 3.2. Impact of hPL coating on cell adhesion

The effect of hPL-coated HA/β-TCP scaffolds on cell adhesion was assessed by DNA quantification (Fig. 2A). The number of hMSC adherent on the scaffold was higher with the hPL coating

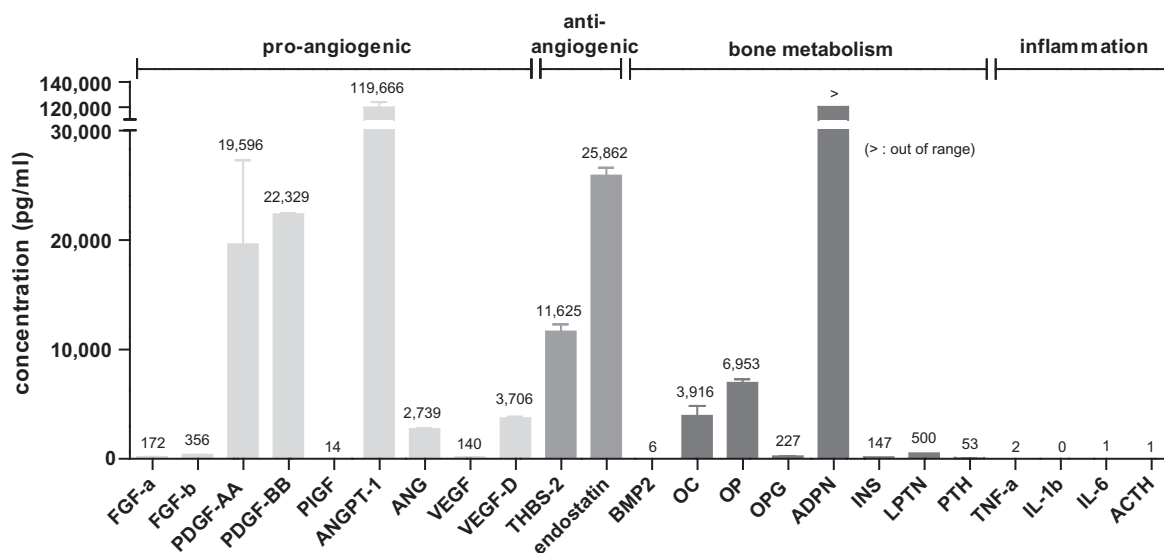
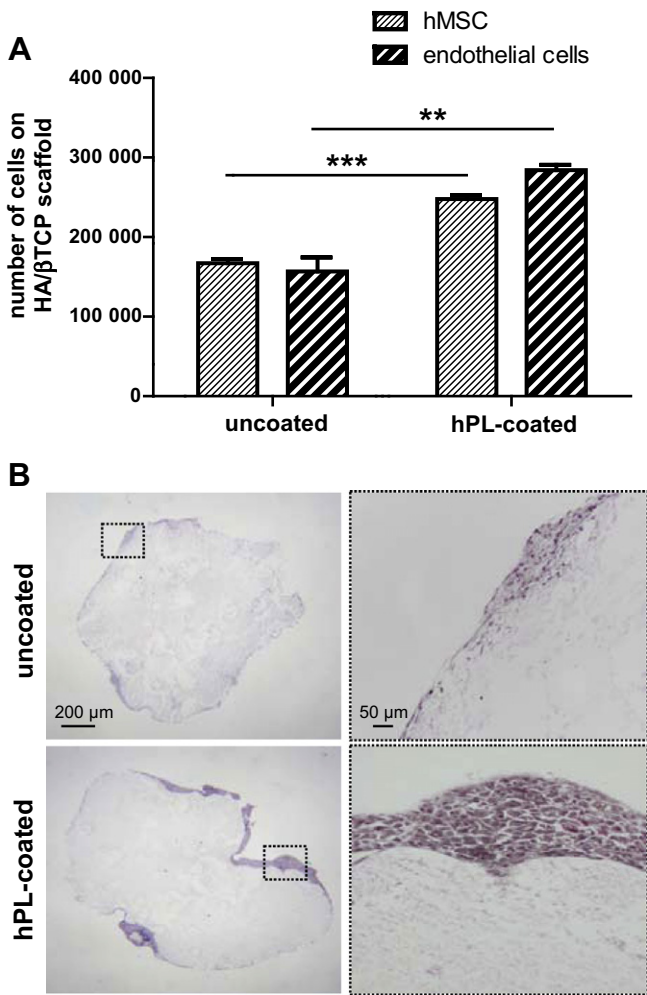


Fig. 1. Assay of protein content of human platelet lysate (hPL), performed using bead-based multiplex analyses. Mean data  $\pm$  SEM.



**Fig. 2.** Cell adhesion on hPL-coated or uncoated HA/ $\beta$ -TCP scaffolds. (A) Quantification of the number of hMSC and endothelial cells on the HA/ $\beta$ -TCP scaffolds, obtained by DNA quantification using Picogreen<sup>®</sup>. (B) Histological analysis 24 h after seeding of hMSC, followed by paraffin embedding and haematoxylin staining. Scale bars as indicated. The dotted line square corresponds to a higher magnification of the area. These analyses were performed on hMSC derived from bone marrow of three different donors ( $n = 6$  scaffolds per condition). \*\*\* $p < 0.001$ .

(248,009  $\pm$  21,446) compared with uncoated scaffolds (167,023  $\pm$  23,243). This result was further confirmed through histological analysis and haematoxylin staining (Fig. 2B), which revealed the formation of a hMSC multilayer, which was thicker when hPL was present. The same experiment was performed with endothelial cells and the number of cells adherent on the hPL-coated HA/ $\beta$ -TCP scaffolds was also greater (284,293  $\pm$  14,510) than those on uncoated scaffolds (156,900  $\pm$  39,648) (Fig. 2A). Taken together, these data indicate that hPL coating significantly increases cell adhesion on HA/ $\beta$ -TCP scaffolds.

### 3.3. Impact of hPL coating on cell morphology and distribution

The effect of hPL-coated HA/ $\beta$ -TCP scaffolds on cell morphology and distribution was evaluated by SEM (Fig. 3). 3 h after seeding ball-shaped hMSC were uniformly distributed across the uncoated scaffold, whereas the hMSC had cytoplasmic extensions similar to pseudopodia when the scaffold was coated with hPL. After 24 h cells showed an elongated shape and were spread over the scaffold under both conditions, but covered it almost entirely in the presence of hPL. 7 days after seeding no differences were observed between hPL-coated and uncoated HA/ $\beta$ -TCP scaffolds, with cells completely covering the biomaterial forming several cell layers. These observations suggest that hPL coating promotes faster adhesion of hMSC to HA/ $\beta$ -TCP scaffolds, affecting their morphology but not their distribution.

### 3.4. Effect of hPL coating on cell migration

Cell migration was assessed by Boyden chamber assay to evaluate the effect of the coating on chemotaxis. This analysis showed that the number of hMSC that migrated through the membrane was significantly higher when the scaffold was coated with hPL, as indicated by the fluorescence intensity (374  $\pm$  676 for uncoated vs. 19,806  $\pm$  1101 for hPL-coated) (Fig. 4A). The same experiment was performed with endothelial cells and hPL coating also significantly increased their migration through the membrane (895  $\pm$  269 for uncoated vs. 2681  $\pm$  520 for hPL-coated) (Fig. 4A). These results were confirmed by nuclear staining of migrated cells present on the underside of the membrane. The number of hMSC and endothelial cells labelled with DAPI was greater for hPL-coated HA/ $\beta$ -TCP scaffolds, indicating that cells migrated

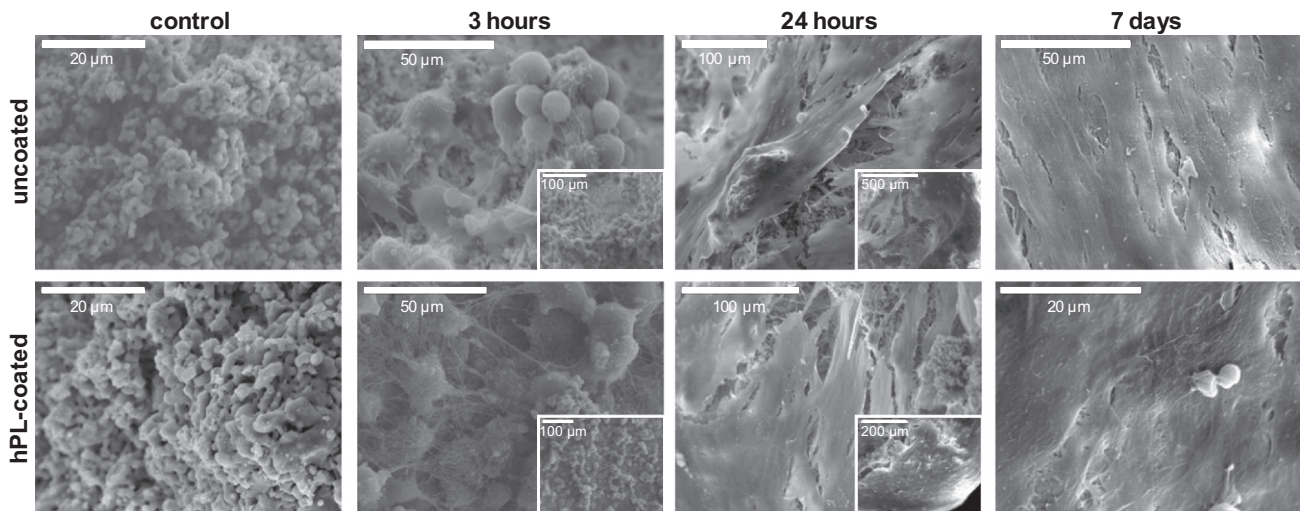


**Fig. 3.** Morphology and distribution of hMSC on hPL-coated and uncoated HA/ $\beta$ -TCP scaffolds, 3 h, 24 h and 7 days after seeding. Constructs were observed by SEM. Scale bars as indicated.

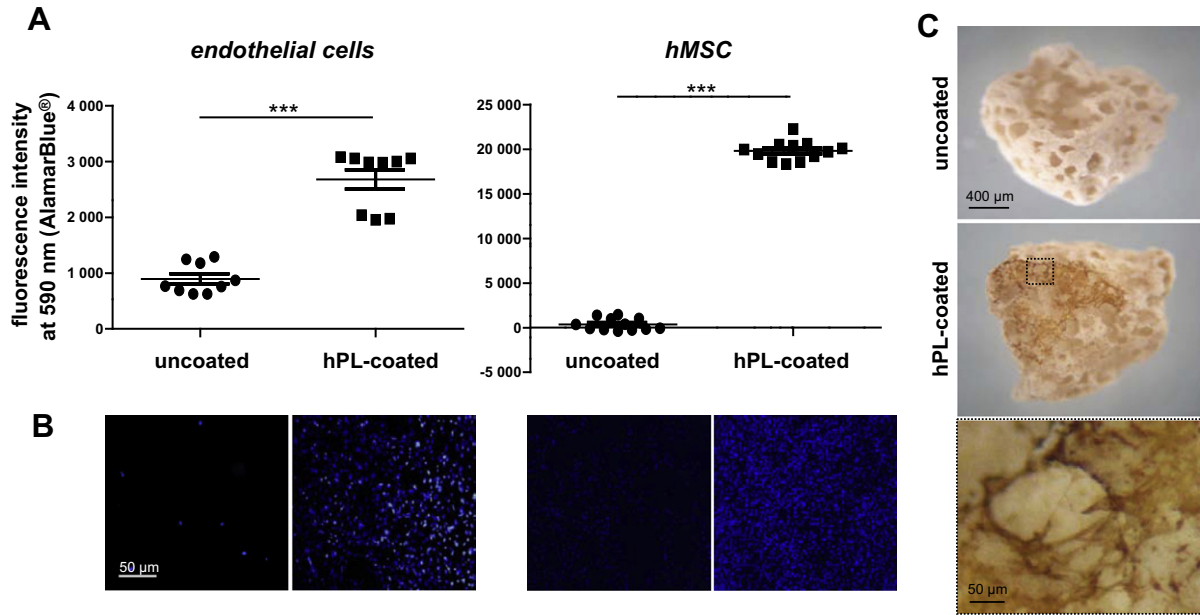


**Fig. 4.** Cell chemo-attraction on hPL-coated and uncoated HA/β-TCP scaffolds. Cell migration was assessed by Boyden chamber assay. (A) The number of endothelial cells and hMSC crossing the membrane was determined using alamarBlue® reagent. The fluorescence is proportional to the number of living cells and corresponds to the metabolic activity of cells that migrated through the membrane. (B) Immunofluorescence analysis of migrated cells by nuclear staining with DAPI (blue). Scale bars as indicated. (C) Evaluation of chemo-attracted hMSC on HA/β-TCP scaffolds by immunohistochemical staining of human β2-microglobulin (brown). Scale bars as indicated. The dotted line square corresponds to a higher magnification of the area. These analyses were performed on hMSC derived from bone marrow of three different donors ( $n = 2$  scaffolds per condition). \*\*\* $p < 0.001$ .

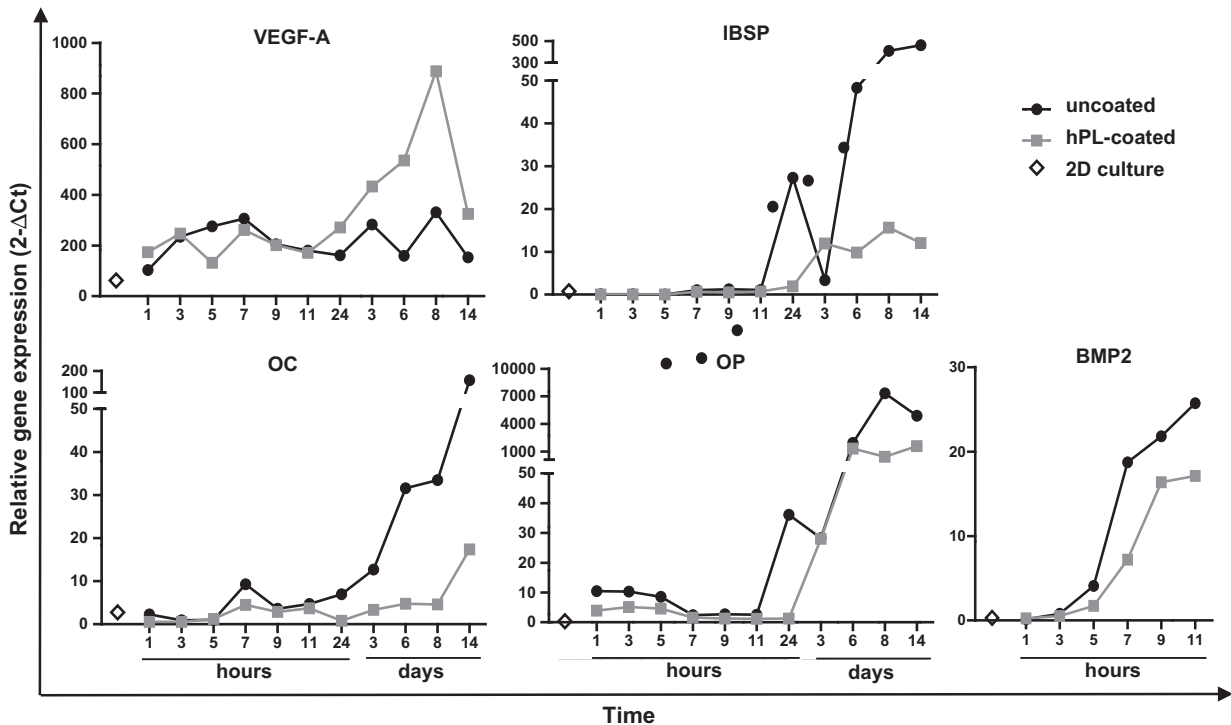


**Fig. 5.** Kinetics of angiogenic (VEGF-A) and osteoblastic (BSP, OC, OP and BMP2) gene expression as determined by RT-qPCR for hMSC in 2-D culture as well as seeded on hPL-coated and uncoated HA/βTCP scaffolds, between 0 and 14 days after seeding. Values for all genes were normalized to GAPDH and results are presented as  $2^{-\Delta Ct}$ . This analysis was performed on hMSC derived from bone marrow ( $n = 2$  scaffolds per condition).

further through the membrane (Fig. 4B). To complete this analysis the chemo-attraction of hMSC and their ability to adhere to bio-materials were evaluated by immunohistochemical staining of human β2-microglobulin (Fig. 4C). This experiment revealed that

hPL coating promotes hMSC migration and adhesion to the scaffold. Moreover, no labelling was visible on the uncoated scaffold, indicating that hPL coating is necessary for hMSC chemo-attraction and adhesion on this biomaterial. Taken together these re-

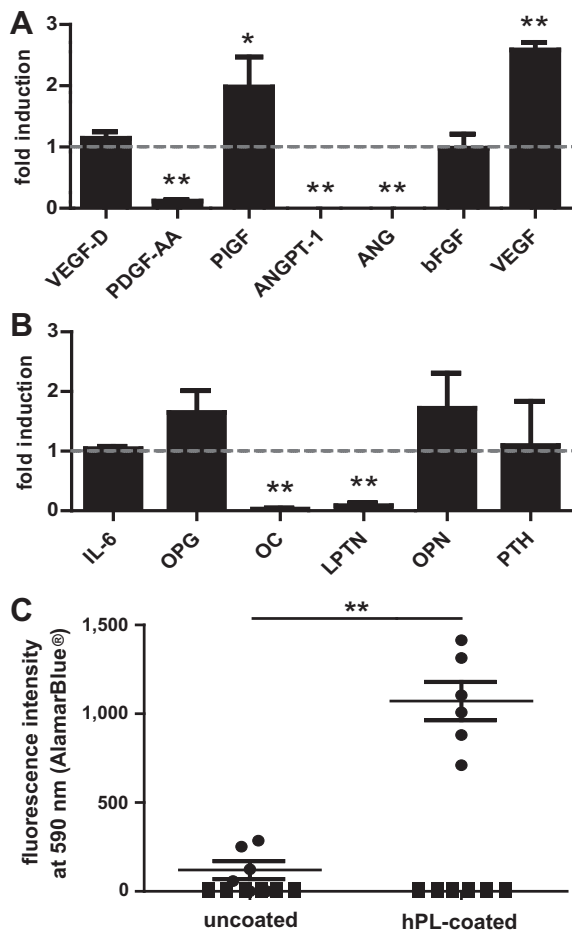


**Fig. 6.** Analysis of secreted proteins by hMSC on hPL-coated and uncoated HA/ $\beta$ -TCP scaffolds and their impact on cell chemoattraction. (A and B) Measurement of proteins secreted by hMSC 7 days after seeding on hPL-coated and uncoated HA/ $\beta$ -TCP scaffolds, (A) for the angiogenic panel and (B) the bone metabolism panel. Results are expressed as fold induction compared with the uncoated condition. Cell-free scaffolds, hPL-coated or uncoated, were used to determine the background. (C) Cell migration of endothelial cells (●) and hMSC (■) assessed by Boyden chamber assay. Chemotaxis was evaluated using hMSC conditioned medium harvested 7 days after seeding on uncoated or hPL-coated HA/ $\beta$ -TCP scaffolds. Cell-free scaffolds, uncoated or hPL-coated, were used to determine the background. The number of cells crossing the membrane was determined using alamarBlue® reagent. The fluorescence is proportional to the number of living cells and corresponds to the metabolic activity of cells that migrated through the membrane. These analyses were performed on hMSC derived from bone marrow of three different donors ( $n = 2$  scaffolds per condition). \* $p < 0.05$ ; \*\* $p < 0.01$ .

sults provide evidence that hPL coating enhances cell migration on HA/ $\beta$ -TCP scaffolds.

### 3.5. Osteoblastic and angiogenic gene expression

Gene expression was analysed in hMSC seeded on HA/ $\beta$ -TCP scaffolds, hPL-coated or uncoated, every 2 h for 12 h and then 1, 3, 6, 8 and 14 days after seeding (Fig. 5). This analysis reveals that seeding hMSC on HA/ $\beta$ -TCP scaffolds up-regulates all gene expression compared with cells grown in two-dimensional culture. However, induction of late osteoblastic genes such as OC, OP, bone sialoprotein 2 (BSP) and bone morphogenetic protein 2 (BMP2) is lower in the presence of hPL. In contrast, hPL coating induces the expression of VEGF-A from 24 h, with peak expression at 8 days (2.68 $\times$  higher expression). This up-regulation seems to decline between 8 and 14 days.

### 3.6. Measurement of proteins secreted by hMSC

To determine the angiogenic and bone metabolism panels of proteins secreted by hMSC conditioned medium was harvested 7 days after seeding on either hPL-coated or uncoated HA/ $\beta$ -TCP scaffolds and measured for protein levels (Fig. 6A and B). Cell-free scaffolds, hPL-coated or uncoated, were used to determine the background levels. Among the panels studied no protein involved in bone metabolism seemed to be up-regulated by the hPL coating, while it induced secretion of two proteins in the angiogenic panel. Thus secretion of PIGF and VEGF was significantly higher when hMSC were seeded on hPL-coated HA/ $\beta$ -TCP scaffolds (1.98- and 2.60-fold induction, respectively). At the same time hPL coating seems significantly inhibit secretion of PDGF-AA, ANGPT-1, ANG, LPTN and OC by hMSC. Furthermore, no secretion of PDGF-BB, interleukin 1 $\beta$ , tumour necrosis factor  $\alpha$ , ACTH, ADPN and INS was detected under either condition. Taken together these results indicate that hPL coating induces the secretion of pro-angiogenic proteins such as PIGF and VEGF by hMSC.

### 3.7. Specific effect of secreted proteins by hMSC on endothelial cells migration

PIGF and VEGF are well-known growth factors involved in endothelial cell migration. Thus the effect of these proteins secreted by hMSC was evaluated on cell chemo-attraction by Boyden chamber assay (Fig. 6C). For this purpose hMSC conditioned medium was harvested 7 days after seeding on hPL-coated or uncoated HA/ $\beta$ -TCP scaffolds. Conditioned medium from hPL-coated or uncoated cell-free scaffolds was used as a control to determine the background cell migration. This analysis showed that the number of endothelial cells that crossed the membrane was significantly higher with conditioned medium of hMSC seeded on hPL-coated HA/ $\beta$ -TCP scaffolds, as indicated by the fluorescence intensity (120  $\pm$  125 for uncoated vs. 1072  $\pm$  264 for hPL-coated). Cell migration studies were also performed with hMSC, but no difference was detected. These results suggest that the hPL coating induces secretion of proteins by hMSC which allow specific chemo-attraction of endothelial cells.

### 3.8. Analysis of in vivo new bone formation

The osteogenic capacity of hMSC seeded on hPL-coated or uncoated HA/ $\beta$ -TCP scaffolds was investigated in vivo using ectopic implantation in immunodeficient SCID mice ( $n = 8$  scaffolds per condition). Cell-free scaffolds were incubated under similar conditions and served as controls ( $n = 3$  scaffolds per condition). 7 weeks post-implantation analysis revealed minimal scaffold resorption and no evidence of mass inflammatory reaction for either scaffold inside the pores of the constructs or in peri-implant tissues (Fig. 7A–C). New bone formation was observed in 37.5% of hMSC-HA/ $\beta$ -TCP scaffolds coated with hPL (Fig. 7A and Table 3). This new tissue contained osteocyte-like cells and osteoblast-like cells lining the surface. For scaffolds with bone formation a quantitative analysis was performed. Compared with the total bone surface area an average of 3.3  $\pm$  1.4% new bone formation was obtained. In contrast, there was no bone formation but only loosely organized connective tissues with hMSC-HA/ $\beta$ -TCP scaffolds without hPL coating (Fig. 7B) and negative controls (Fig. 7C). These results demonstrate that hMSC seeded on hPL-coated HA/ $\beta$ -TCP scaffolds improve in vivo new bone formation.

### 3.9. Analysis of in vivo neovascularization

In the light of the results obtained in vitro on endothelial cell chemo-attraction and the difference in in vivo bone formation, neovascularization of implants was studied 2 weeks post-implan-

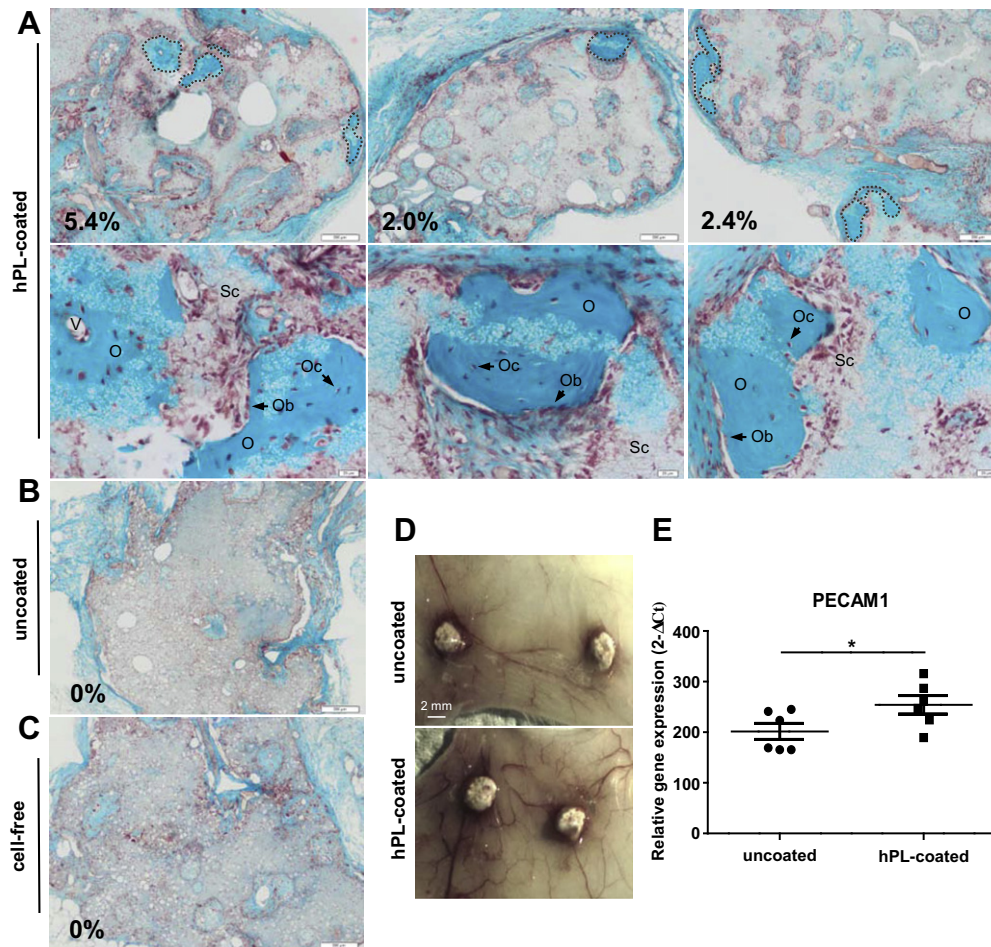


**Fig. 7.** Analysis of in vivo new bone formation and neovascularization after ectopic implantation of hPL-coated (A and C) or uncoated (B) HA/ $\beta$ -TCP, seeded with hMSC (A and B) or not seeded (cell-free) (C), in immunodeficient SCID mice for 2 (D, E) or 7 (A–C) weeks. (A–C) Histological analysis of new bone formation after decalcification and Masson’s Trichrome staining (blue/green, collagen and bone; purple, nuclei; pink, cytoplasm). Dotted lines correspond to the areas of new bone formation. The percentage of new bone formation area compared with the total scaffold area is indicated in the bottom left corner. (A) Higher magnifications are presented for each hPL-coated HA/ $\beta$ -TCP scaffold on the lower line. O, osteoid; Oc, osteocyte; Ob, osteoblast; Sc, scaffold; V, blood vessel. Scale bars: as indicated. (D) Macroscopic observation of in vivo vascularization of implants containing hMSC. Scale bars as indicated. (E) Relative gene expression of mouse PECAM1 as determined by RT-qPCR for hMSC seeded on hPL-coated and uncoated HA/ $\beta$ -TCP scaffolds. Values were normalized to GAPDH and results are presented as  $2^{-\Delta\Delta Ct}$ . These analyses were performed on hMSC derived from bone marrow of one donor ( $n = 8$  scaffolds per condition for (A) and (B);  $n = 3$  cell-free scaffolds per condition for (C);  $n = 3$  scaffolds per condition for (D) and (E)). \* $p < 0.05$ .

**Table 3**  
Frequency of ectopic new bone formation.

hMSC–HA/ $\beta$ -TCP	No. of scaffolds with new bone formation
Uncoated	0/8
hPL-coated	3/8

tation ( $n = 3$  scaffolds per condition). Cell-free scaffolds were incubated under similar conditions and served as controls ( $n = 3$  scaffolds per condition). This observation showed the presence of blood vessels around hMSC-HA/ $\beta$ -TCP scaffolds under both conditions, but in greater numbers with hPL coating (Fig. 7D). In order to quantify implant neovascularization the expression of a mouse vascular endothelial marker, PECAM1, was analysed (Fig. 7E). Higher expression of the mouse PECAM1 gene was observed for hMSC-HA/ $\beta$ -TCP scaffolds coated with hPL, confirming the above results. Taken together these data suggest that hPL coating enhances in vivo neovascularization of hMSC-HA/ $\beta$ -TCP scaffolds.

**4. Discussion**

Tissue regeneration is a complex process that requires activation, migration, proliferation and differentiation of multiple cell

types that ensure extracellular matrix synthesis and formation of different morphological structures. This process is regulated by a cascade of signals, including a number of molecules such as growth factors. The coordinated action of progenitor cells, release of growth factors, vascularization of the de novo tissue and a suitable scaffold template are essential for successful bone regeneration. hPL is composed of many growth factors known for their proliferative, differentiative and chemo-attractive effects on various cells involved in wound healing and bone growth. As we had previously shown the potential of hPL medium to enhance hMSC osteogenic differentiation [22] we designed a new strategy of coating HA/ $\beta$ -TCP scaffolds with hPL to potentiate the biomaterial’s regenerative properties in order to induce the rapid development of a vascular network and optimize the process of bone repair. In this study we have demonstrated that hPL can be coated on HA/ $\beta$ -TCP scaffolds, directly increasing chemo-attraction and colonization of the scaffolds by stem cells, as well as stimulating the paracrine activity of hMSC, resulting in an improvement in vascularization and bone formation after in vivo ectopic implantation.

To reach the site of injury and initiate the healing process cells have to migrate to the target area. This migratory activity can be mediated by chemokines and is important in therapeutic approaches. Platelets have been shown to accumulate and release a



variety of potent chemotactic factors that induce the recruitment of various cells such as bone marrow-derived progenitor cells [39] and EPC [40–42]. This suggests their potential use in medicine to facilitate tissue regeneration [43]. Our results demonstrate that hPL-coated HA/ $\beta$ -TCP scaffolds clearly enhance chemoattraction of hMSC and endothelial cells through a membrane. Their migration and adhesion to the scaffold could be related to a significant number of growth factors contained in hPL known for their role in cell mobilization. Indeed, our protein analysis reveals the presence of many growth factors naturally found in healthy bone matrix or expressed during fracture healing to ensure tissue development, for example vascularization and differentiation of osteoprogenitor cells. Among them were PDGF-AA, PDGF-BB, ANG, ANGPT-1, VEGF-D, VEGF, aFGF, bFGF, THBS-2, endostatin, OC, OP, ADPN, OPG, LPTN and INS [9,44–49]. Some of these factors have been specifically described in the literature as having a role in cell recruitment. Platelet-derived bFGF has been shown to promote and control migration of hMSC [50,51]. It has also been demonstrated that PDGF stimulates hMSC migration [23], as does VEGF, by binding to and activating PDGF receptors [52]. Stromal cell-derived factor-1 (SDF-1) is also secreted by platelets [39] and seems to mediate the trafficking of rat MSC into sites of brain injury [53]. Chemokines such as VEGF, SDF-1 and ANGPT-1 are also known to mobilize other cell types, such as progenitor cells [54,55], endothelial cells [56] and mature osteoblasts [57]. Other growth, like TGF- $\beta$  and IGF, have been shown to be contained in hPL [20,21] and have been shown to have a role in bone repair [44]. All these factors contribute to tissue homeostasis, providing the balance between stimulating and inhibiting factors required for angiogenesis and bone remodelling [8,47,58]. Taken together these findings suggest that hPL can induce the recruitment of resident stem/progenitor cells or mature cells which could participate in the development of tissue-engineered bone *in vivo*.

We used an ectopic model to investigate the *in vivo* effect of hPL coating on the bone formation capacity of hMSC. We have previously shown the low potential for bone formation of hMSC grown in standard growth medium complemented with FBS [22], and no bone formation was found when scaffolds were uncoated. New bone formation was observed only with hMSC-HA/ $\beta$ -TCP scaffolds coated with hPL. These findings *in vivo* are consistent with the positive role of hPL in bone repair that we and others have previously reported [22,35]. Surprisingly, in contrast to hPL used as a culture supplement, our *in vitro* results indicate that hPL coated on biomaterials does not induce osteoblastic gene or protein expression by hMSC. Inhibition of BSP and OC was even observed in under 3-D conditions. The absence of osteoinduction could be due to insufficient adhesion or the concentration or stability of osteoinductive proteins such as BMP2, which is present at only very low levels in hPL (6 pg ml<sup>-1</sup>) on the scaffold. However, it is possible that hMSC self-regulates the secretion of OC, which is already present in hPL. In spite of this lack of osteoblastic induction *in vitro*, hPL coating may still play a role on grafted hMSC osteoblastic differentiation *in vivo*, as new bone formation occurs. Two distinct mechanisms of action of implanted cells have been described [59]. Differentiated cells could participate directly by forming new bone, whereas undifferentiated cells act indirectly by recruiting endogenous cells to restore damaged tissues. In our study hMSC released paracrine factors which may act on host cells. This hypothesis is supported by the demonstration that *in vitro* hPL coating induced the expression of pro-angiogenic factors such as VEGF and PlGF by hMSC at the mRNA and/or protein levels. The induction of VEGF gene expression can be explained by the presence of the positive regulators EGF, TGF- $\beta$ , IGF-1, FGF and PDGF in hPL [60,61]. VEGF and PlGF are members of the VEGF family, which stimulate angiogenesis through growth, mobilization and differentiation of EPC [62–64]. Thus we confirmed their effect on cell migration with

*in vitro* chemotaxis assay which highlights specific enhancement of the chemoattractive activity mediated by hMSC-seeded HA/ $\beta$ -TCP scaffolds coated with hPL on endothelial cells. Analysis of implant vascularization *in vivo* supports the hypothesis of a paracrine role of hMSC-HA/ $\beta$ -TCP scaffolds coated with hPL on endothelial cells, since this condition presents a greater number of blood vessels and enhanced expression of the vascular endothelial marker mouse PECAM-1. At the same time we observed inhibition of PDGF-AA, ANGPT-1 and ANG secretion by hMSC on hPL-coated HA/ $\beta$ -TCP scaffolds. It is possible that hMSC self-regulate the secretion of these pro-angiogenic proteins which are already present in large amounts in hPL. These results indicate that hPL coating induces the secretion of PlGF and VEGF by hMSC *in vitro*, which likely allows the specific recruitment and proliferation of endogenous endothelial cells participating in blood vessel formation *in vivo*. Then ANGPT-1 and ANG, present in large amounts in hPL, will stimulate vascular remodelling.

It has been shown that cell number is directly linked to bone formation [65]. As we have demonstrated that hPL coating provides improved cell adhesion on HA/ $\beta$ -TCP scaffolds another hypothesis is that bone regeneration is due to this greater number of cells. This higher number of hMSC on hPL-coated HA/ $\beta$ -TCP scaffolds could be explained by the release from platelets granules of adhesive proteins involved in homeostasis, such as fibronectin and fibrinogen [66]. The results of SEM analyses confirm that HA/ $\beta$ -TCP scaffolds coated with hPL provide a suitable 3-D environment for cell adhesion. Indeed, the pseudopodia observed by SEM indicate the formation of focal adhesions between cells and the hPL matrix permitting rapid and adequate distribution of hMSC. Moreover, hPL contains a large number of growth factors, such as PDGF, EGF, TGF- $\beta$ , bFGF and IGF-1, known for their role in cell proliferation [67–69]. Effectively, we and others have shown that hPL enhances hMSC expansion *in vitro* [22]. These growth factors which play a role in cell proliferation may also contribute to improved bone formation.

Our results confirm the positive effect of hPL on bone regeneration. Our results also mechanistically explain the role of hPL in tissue regeneration. It increases cell adhesion and drives host cell recruitment, directly or indirectly, through a paracrine effect of implanted hMSC, which participate in vascularization and bone healing. hPL seems a promising candidate for potentiating biomaterial regenerative properties and developing a novel clinical strategy for bone repair. To obtain optimal bone regeneration it would be interesting to optimize the coating system. Our current strategy only allows outer coating of the biomaterial. In order to enhance cell penetration the use of hPL perfusion inside the scaffold could be a solution. On the other hand, the development of a delivery system which could release hPL precisely at an adequate concentration would provide a significant increase in bone formation. The presentation of multiple growth factors, released at appropriate intervals from 3-D biodegradable scaffolds offers an attractive strategy for improving bone repair, mimicking the *in vivo* environment and wound healing.

## 5. Conclusions

In this study we have reported that functionalizing HA/ $\beta$ -TCP scaffolds with hPL combined with hMSC improves bone tissue engineering. Indeed, using a murine ectopic model we showed that hPL coating enhances *in vivo* neovascularization and bone formation. hPL potentiates the biomaterial regenerative properties, inducing improved adhesion and a more rapid colonization of the scaffold by stem cells. It also drives host cell recruitment, directly or indirectly, through a paracrine effect of the implanted cells. We have previously shown that the soluble form of hPL enhances

hMSC proliferation and primes hMSC differentiation towards the osteoblastic lineage, which enhances *in vivo* bone regeneration, thus the use of cells grown in hPL could act synergistically with hPL-coated scaffolds. Moreover, growing cells in FBS is becoming more and more unattractive for clinical use due to safety reasons, such as pathogen transmission and immunogenicity. Our findings provide evidence of the potential of hPL to functionalize biomaterials and in particular to develop novel clinical strategies for bone repair.

### Acknowledgements

This work was partially supported by EFS Ile de France and by the 7th Framework Program of the European Commission through the project REBORNE no. 241879. J.L. was supported by the DIM-STEM-Pôle Ile-de-France. We would like to thank the Centre de Recherches Chirurgicales Dominique Chopin for the use of their animal platform facilities. We are grateful to the company Ceraver, which kindly provided the ceramics, as well the laboratories of Dr Llorens-Cortes and Dr Li, which provided endothelial cells. We thank the SEM platform of the Université Paris-Est and the luminex platform of IMRB, with special thanks to Patrick Ausset and Mathieu Surenaud, respectively, for their help. We also thank Angélique Lebouvier, Grégory Franck and Nicolas Jullien for their critical review of the manuscript.

### Appendix A. Figures with essential colour discrimination

Certain figures in this article, particularly Figs. 2, 4, 7 are difficult to interpret in black and white. The full colour images can be found in the on-line version, at <http://dx.doi.org/10.1016/j.actbio.2013.02.003>.

### References

- [1] Langer R, Vacanti JP. Tissue engineering. *Science* 1993;260(5110):920–6.
- [2] Einhorn TA. Enhancement of fracture-healing. *J Bone Joint Surg Am* 1995;77(6):940–56.
- [3] Dimitriou R, Jones E, McGonagle D, Giannoudis PV. Bone regeneration: current concepts and future directions. *BMC Med* 2011;9:66.
- [4] Bruder SP, Kraus KH, Goldberg VM, Kadiyala S. The effect of implants loaded with autologous mesenchymal stem cells on the healing of canine segmental bone defects. *J Bone Joint Surg Am* 1998;80(7):985–96.
- [5] Petite H, Viateau V, Bensaid W, Meunier A, de Pollak C, Bourguignon M, et al. Tissue-engineered bone regeneration. *Nat Biotechnol* 2000;18(9):959–63.
- [6] Kon E, Muraglia A, Corsi A, Bianco P, Marcacci M, Martin I, et al. Autologous bone marrow stromal cells loaded onto porous hydroxyapatite ceramic accelerate bone repair in critical-size defects of sheep long bones. *J Biomed Mater Res* 2000;49(3):328–37.
- [7] Coquelin L, Fialaire-Legendre A, Roux S, Poignard A, Bierling P, Hernigou P, et al. *In vivo* and *in vitro* comparison of three different allografts vitalized with human mesenchymal stromal cells. *Tissue Eng Part A* 2012;18(17–18):1921–31.
- [8] Fernandez-Tresguerres-Hernandez-Gil I, Alobera-Gracia MA, Del-Canto-Pingarron M, Blanco-Jerez L. Physiological bases of bone regeneration I. Histology and physiology of bone tissue. *Med Oral Patol Oral Cir Bucal* 2006;11(1):E47–51.
- [9] Deschaseaux F, Sensebe L, Heymann D. Mechanisms of bone repair and regeneration. *Trends Mol Med* 2009;15(9):417–29.
- [10] Carano RA, Filvaroff EH. Angiogenesis and bone repair. *Drug Discov Today* 2003;8(21):980–9.
- [11] Fang TD, Salim A, Xia W, Nacamuli RP, Guccione S, Song HM, et al. Angiogenesis is required for successful bone induction during distraction osteogenesis. *J Bone Miner Res* 2005;20(7):1114–24.
- [12] Kanczler JM, Oreffo RO. Osteogenesis and angiogenesis: the potential for engineering bone. *Eur Cell Mater* 2008;15:100–14.
- [13] Yu H, VandeVord PJ, Mao L, Matthew HW, Woolley PH, Yang SY. Improved tissue-engineered bone regeneration by endothelial cell mediated vascularization. *Biomaterials* 2009;30(4):508–17.
- [14] Schimming R, Schmelzeisen R. Tissue-engineered bone for maxillary sinus augmentation. *J Oral Maxillofac Surg* 2004;62(6):724–9.
- [15] McCracken M, Lemons JE, Zinn K. Analysis of Ti-6Al-4V implants placed with fibroblast growth factor 1 in rat tibiae. *Int J Oral Maxillofac Implants* 2001;16(4):495–502.
- [16] Srouji S, Blumenfeld I, Rachmiel A, Livne E. Bone defect repair in rat tibia by TGF-beta1 and IGF-1 released from hydrogel scaffold. *Cell Tissue Bank* 2004;5(4):223–30.
- [17] Huang YC, Kaigler D, Rice KG, Krebsbach PH, Mooney DJ. Combined angiogenic and osteogenic factor delivery enhances bone marrow stromal cell-driven bone regeneration. *J Bone Miner Res* 2005;20(5):848–57.
- [18] Kanczler JM, Ginty PJ, White L, Clarke NM, Howdle SM, Shakesheff KM, et al. The effect of the delivery of vascular endothelial growth factor and bone morphogenic protein-2 to osteoprogenitor cell populations on bone formation. *Biomaterials* 2010;31(6):1242–50.
- [19] Tsurushima H, Marushima A, Suzuki K, Oyane A, Sogo Y, Nakamura K, et al. Enhanced bone formation using hydroxyapatite ceramic coated with fibroblast growth factor-2. *Acta Biomater* 2010;6(7):2751–9.
- [20] Frechette JP, Martineau I, Gagnon G. Platelet-rich plasmas: growth factor content and roles in wound healing. *J Dent Res* 2005;84(5):434–9.
- [21] van den Dolder J, Mooren R, Vloon AP, Stoeltinga PJ, Jansen JA. Platelet-rich plasma: quantification of growth factor levels and the effect on growth and differentiation of rat bone marrow cells. *Tissue Eng* 2006;12(11):3067–73.
- [22] Chevallier N, Anagnostou F, Zilber S, Bodivit G, Maurin S, Barrault A, et al. Osteoblastic differentiation of human mesenchymal stem cells with platelet lysate. *Biomaterials* 2010;31(2):270–8.
- [23] Kilian O, Flesch I, Wenisch S, Taborski B, Jork A, Schnettler R, et al. Effects of platelet growth factors on human mesenchymal stem cells and human endothelial cells *in vitro*. *Eur J Med Res* 2004;9(7):337–44.
- [24] Marx RE, Carlson ER, Eichstaedt RM, Schimmele SR, Strauss JE, Georgeff KR. Platelet-rich plasma: growth factor enhancement for bone grafts. *Oral Surg Oral Med Oral Pathol Oral Radiol Endod* 1998;85(6):638–46.
- [25] Kassolis JD, Rosen PS, Reynolds MA. Alveolar ridge and sinus augmentation utilizing platelet-rich plasma in combination with freeze-dried bone allograft: case series. *J Periodontol* 2000;71(10):1654–61.
- [26] Robiony M, Polini F, Costa F, Politi M. Osteogenesis distraction and platelet-rich plasma for bone restoration of the severely atrophic mandible: preliminary results. *J Oral Maxillofac Surg* 2002;60(6):630–5.
- [27] Maiorana C, Sommariva L, Brivio P, Sigurta D, Santoro F. Maxillary sinus augmentation with anorganic bovine bone (Bio-Oss) and autologous platelet-rich plasma: preliminary clinical and histologic evaluations. *Int J Periodontics Restorative Dent* 2003;23(3):227–35.
- [28] Kassolis JD, Reynolds MA. Evaluation of the adjunctive benefits of platelet-rich plasma in subantral sinus augmentation. *J Craniofac Surg* 2005;16(2):280–7.
- [29] Robiony M, Zorzan E, Polini F, Sembronio S, Toro C, Politi M. Osteogenesis distraction and platelet-rich plasma: combined use in restoration of severe atrophic mandible. Long-term results. *Clin Oral Implants Res* 2008;19(11):1202–10.
- [30] Chiang CC, Su CY, Huang CK, Chen WM, Chen TH, Tzeng YH. Early experience and results of bone graft enriched with autologous platelet gel for recalcitrant nonunions of lower extremity. *J Trauma* 2007;63(3):655–61.
- [31] Smrke D, Gubina B, Domanovic D, Rozman P. Allogeneic platelet gel with autologous cancellous bone graft for the treatment of a large bone defect. *Eur Surg Res* 2007;39(3):170–4.
- [32] Dallari D, Savarino L, Stagni C, Cenni E, Cenacchi A, Fornasari PM, et al. Enhanced tibial osteotomy healing with use of bone grafts supplemented with platelet gel or platelet gel and bone marrow stromal cells. *J Bone Joint Surg Am* 2007;89(11):2413–20.
- [33] Doucet C, Ernou I, Zhang Y, Llense JR, Begot L, Holy X, et al. Platelet lysates promote mesenchymal stem cell expansion: a safety substitute for animal serum in cell-based therapy applications. *J Cell Physiol* 2005;205(2):228–36.
- [34] Capelli C, Domenghini M, Borleri G, Bellavita P, Poma R, Carobbio A, et al. Human platelet lysate allows expansion and clinical grade production of mesenchymal stromal cells from small samples of bone marrow aspirates or marrow filter washouts. *Bone Marrow Transplant* 2007;40(8):785–91.
- [35] Salvade A, Della Mina P, Gaddi D, Gatto F, Villa A, Bigoni M, et al. Characterization of platelet lysate cultured mesenchymal stromal cells and their potential use in tissue-engineered osteogenic devices for the treatment of bone defects. *Tissue Eng Part C Methods* 2010;16(2):201–14.
- [36] Reinisch A, Hofmann NA, Obenauf AC, Kaschoer K, Rohde E, Schallmoser K, et al. Humanized large-scale expanded endothelial colony-forming cells function *in vitro* and *in vivo*. *Blood* 2009;113(26):6716–25.
- [37] Dozza B, Di Bella C, Lucarelli E, Giavaresi G, Fini M, Tazzari PL, et al. Mesenchymal stem cells and platelet lysate in fibrin or collagen scaffold promote non-cemented hip prosthesis integration. *J Orthop Res* 2011;29(6):961–8.
- [38] Schweitzer KM, Vicart P, Delouis C, Paulin D, Drager AM, Langenhuijzen MM, et al. Characterization of a newly established human bone marrow endothelial cell line: distinct adhesive properties for hematopoietic progenitors compared with human umbilical vein endothelial cells. *Lab Invest* 1997;76(1):25–36.
- [39] Massberg S, Konrad I, Schurzinger K, Lorenz M, Schneider S, Zohlnhofer D, et al. Platelets secrete stromal cell-derived factor 1alpha and recruit bone marrow-derived progenitor cells to arterial thrombi *in vivo*. *J Exp Med* 2006;203(5):1221–33.
- [40] Langer H, May AE, Daub K, Heinzmann U, Lang P, Schumm M, et al. Adherent platelets recruit and induce differentiation of murine embryonic endothelial progenitor cells to mature endothelial cells *in vitro*. *Circ Res* 2006;98(2):e2–e10.
- [41] de Boer HC, Verseyden C, Ulfman LH, Zwaginga JJ, Bot I, Biessen EA, et al. Fibrin and activated platelets cooperatively guide stem cells to a vascular injury and promote differentiation towards an endothelial cell phenotype. *Arterioscler Thromb Vasc Biol* 2006;26(7):1653–9.
- [42] Lev El, Estrov Z, Aboulfatova K, Harris D, Granada JF, Alviar C, et al. Potential role of activated platelets in homing of human endothelial progenitor cells to subendothelial matrix. *Thromb Haemost* 2006;96(4):498–504.

- [43] Langer HF, Gawaz M. Platelets in regenerative medicine. *Basic Res Cardiol* 2008;103(4):299–307.
- [44] Lieberman JR, Daluiski A, Einhorn TA. The role of growth factors in the repair of bone. Biology and clinical applications. *J Bone Joint Surg Am* 2002;84-A(6):1032–44.
- [45] Coen G. Leptin and bone metabolism. *J Nephrol* 2004;17(2):187–9.
- [46] Oshima K, Nampei A, Matsuda M, Iwaki M, Fukuhara A, Hashimoto J, et al. Adiponectin increases bone mass by suppressing osteoclast and activating osteoblast. *Biochem Biophys Res Commun* 2005;331(2):520–6.
- [47] Karamysheva AF. Mechanisms of angiogenesis. *Biochemistry (Mosc)* 2008;73(7):751–62.
- [48] Tanaka H, Mine T, Ogasa H, Taguchi T, Liang CT. Expression of RANKL/OPG during bone remodeling in vivo. *Biochem Biophys Res Commun* 2011;411(4):690–4.
- [49] Hou CJ, Liu JL, Li X, Bi LJ. Insulin promotes bone formation in augmented maxillary sinus in diabetic rabbits. *Int J Oral Maxillofac Surg* 2011;41(3):400–7.
- [50] Schmidt A, Ladage D, Schinkothe T, Klausmann U, Ulrichs C, Klinz FJ, et al. Basic fibroblast growth factor controls migration in human mesenchymal stem cells. *Stem Cells* 2006;24(7):1750–8.
- [51] Langer HF, Stellos K, Steingen C, Frohofer A, Schonberger T, Kramer B, et al. Platelet derived bFGF mediates vascular integrative mechanisms of mesenchymal stem cells in vitro. *J Mol Cell Cardiol* 2009;47(2):315–25.
- [52] Ball SG, Shuttleworth CA, Kielty CM. Vascular endothelial growth factor can signal through platelet-derived growth factor receptors. *J Cell Biol* 2007;177(3):489–500.
- [53] Ji JF, He BP, Dheen ST, Tay SS. Interactions of chemokines and chemokine receptors mediate the migration of mesenchymal stem cells to the impaired site in the brain after hypoglossal nerve injury. *Stem Cells* 2004;22(3):415–27.
- [54] Moore MA, Hattori K, Heissig B, Shieh JH, Dias S, Crystal RG, et al. Mobilization of endothelial and hematopoietic stem and progenitor cells by adenovector-mediated elevation of serum levels of SDF-1, VEGF, and angiopoietin-1. *Ann NY Acad Sci* 2001;938:36–45.
- [55] Heil M, Mitnacht-Krauss R, Issbrucker K, van den Heuvel J, Dehio C, Schaper W, et al. An engineered heparin-binding form of VEGF-E (hbVEGF-E). Biological effects in vitro and mobilization of precursor cells. *Angiogenesis* 2003;6(3):201–11.
- [56] Witznitchler B, Maisonpierre PC, Jones P, Yancopoulos GD, Isner JM. Chemotactic properties of angiopoietin-1 and -2, ligands for the endothelial-specific receptor tyrosine kinase Tie2. *J Biol Chem* 1998;273(29):18514–21.
- [57] Mayr-Wohlfart U, Waltenberger J, Hausser H, Kessler S, Gunther KP, Dehio C, et al. Vascular endothelial growth factor stimulates chemotactic migration of primary human osteoblasts. *Bone* 2002;30(3):472–7.
- [58] Italiano Jr JE, Richardson JL, Patel-Hett S, Battinelli E, Zaslavsky A, Short S, et al. Angiogenesis is regulated by a novel mechanism: pro- and antiangiogenic proteins are organized into separate platelet alpha granules and differentially released. *Blood* 2008;111(3):1227–33.
- [59] Tortelli F, Tasso R, Loiacono F, Cancedda R. The development of tissue-engineered bone of different origin through endochondral and intramembranous ossification following the implantation of mesenchymal stem cells and osteoblasts in a murine model. *Biomaterials* 2010;31(2):242–9.
- [60] Ferrara N, Davis-Smyth T. The biology of vascular endothelial growth factor. *Endocr Rev* 1997;18(1):4–25.
- [61] Neufeld G, Cohen T, Gengrinovitch S, Poltorak Z. Vascular endothelial growth factor (VEGF) and its receptors. *FASEB J* 1999;13(1):9–22.
- [62] Asahara T, Takahashi T, Masuda H, Kalka C, Chen D, Iwaguro H, et al. VEGF contributes to postnatal neovascularization by mobilizing bone marrow-derived endothelial progenitor cells. *EMBO J* 1999;18(14):3964–72.
- [63] Yu JX, Huang XF, Lv WM, Ye CS, Peng XZ, Zhang H, et al. Combination of stromal-derived factor-1alpha and vascular endothelial growth factor gene-modified endothelial progenitor cells is more effective for ischemic neovascularization. *J Vasc Surg* 2009;50(3):608–16.
- [64] De Falco S. The discovery of placenta growth factor and its biological activity. *Exp Mol Med* 2012;44(1):1–9.
- [65] Mankani MH, Kuznetsov SA, Robey PG. Formation of hematopoietic territories and bone by transplanted human bone marrow stromal cells requires a critical cell density. *Exp Hematol* 2007;35(6):995–1004.
- [66] Muller AM, Davenport M, Verrier S, Drosner R, Alini M, Bocelli-Tyndall C, et al. Platelet lysate as a serum substitute for 2D static and 3D perfusion culture of stromal vascular fraction cells from human adipose tissue. *Tissue Eng Part A* 2009;15(4):869–75.
- [67] Gronthos S, Simmons PJ. The growth factor requirements of STRO-1-positive human bone marrow stromal precursors under serum-deprived conditions in vitro. *Blood* 1995;85(4):929–40.
- [68] Cassiede P, Dennis JE, Ma F, Caplan AL. Osteochondrogenic potential of marrow mesenchymal progenitor cells exposed to TGF-beta 1 or PDGF-BB as assayed in vivo and in vitro. *J Bone Miner Res* 1996;11(9):1264–73.
- [69] Martin I, Muraglia A, Campanile G, Cancedda R, Quarto R. Fibroblast growth factor-2 supports ex vivo expansion and maintenance of osteogenic precursors from human bone marrow. *Endocrinology* 1997;138(10):4456–62.